Chapter 9

Autoradiography Assessment of Muscarinic Receptors in the Central Nervous System

Vladimir Farar and Jaromir Myslivecek

Abstract

The detection of muscarinic receptor binding sites is a crucial step in many experimental conditions. Although in peripheral tissue, the radioligand binding (see appropriate chapter) allows to obtain well-defined receptor characteristic, and also is usable in some central nervous system regions, when trying to determine receptor binding in central nervous system regions with low density or with infinitesimally small receptor changes, the receptor autoradiography is a better method. The development of this method made important progress, and some different modes (phosphor imaging) are used nowadays. Here, we describe muscarinic receptor detection using different radioligands: [^{3}H]-QNB, [^{3}H]-NMS, [^{3}H]-pirenzepine, and [^{3}H]-AFDX-384. Specific attention is paid to the detection of subtypes of muscarinic receptors and the limits of the method are emphasized.

Key words Muscarinic receptors, Autoradiography, [^{3}H]-QNB, [^{3}H]-NMS, [^{3}H]-pirenzepine, [^{3}H]-AFDX-384, Central nervous system

Abbreviations

^{3}H-QNB	^{3}H-quinuclidinyl benzilate, ^{3}H-1-azabicyclo[2.2.2]oct-3-yl 2-hydroxy-2,2-diphenylacetate
^{3}H-NMS	^{3}H-*N*-methyl-scopolamine, ^{3}H-(1R,2S,4R,5S,7R)-{[(2R)-3-hydroxy-2-phenylpropanoyl]oxy}s[19]-9,9-dimethyl-3-oxa-9-azoniatricyclo[3.3.1.02,4]nonane
^{3}H-pirenzepine	^{3}H-11-[(4-methylpiperazin-1-yl)acetyl]-5,11-dihydro-6H-pyrido[2,3-b][1,4]benzodiazepin-6-one
^{3}H-AFDX-384	^{3}H-*N*-(2-[(2R)-2-[(dipropylamino)methyl]piperidin-1-yl]ethyl)-6-oxo-5H-pyrido[2,3-b][1,4]benzodiazepine-11-carboxamide
RT	Room temperature
MRs	Muscarinic receptors
GPCRs	G protein-coupled receptors

Jaromir Myslivecek and Jan Jakubik (eds.), *Muscarinic Receptor: From Structure to Animal Models*, Neuromethods, vol. 107,
DOI 10.1007/978-1-4939-2858-3_9,

1 Historical Overview

Autoradiography is not a single method, but refers to a general concept shared by a family of experimental techniques. The aim of autoradiography is to visualize and quantify the distribution of radioactive substance within the specimen (e.g., acrylamide gels, agarose gels, nitrocellulose sheets, paper chromatograms, thin layer chromatograms, tissue sections) [1–3]. In principle, the binding of radioactive substance to specific target is not different from radioligand binding (*see* Chapter 3). The radiolabeled compound that is specific to a given receptor is allowed to bind to the receptor and then free radioligand is separated. The first autoradiography screen appeared accidentally when blackening was obtained on silver chloride (and iodide) emulsions (on a photographic plate) by uranium salts (uranium nitrate) [4]. This study and the subsequent work of Henri Becquerel and the Curies (1898) led to the discovery of radioactivity. However, the development of method as a technique to study biological structures became possible only after World War II when photographic emulsions became widely available [5].

Autoradiography technique is able to identify not only proteins but also nucleic acid fragments and can be used in polyacrylamide or agarose gel electrophoresis, in situ hybridization and in subcellular localization of radioactive drug product [1, 3, 6, 7].

One of the first review summarizing pioneering work using acetylcholine receptor imaging was study [8] in which nicotinic acetylcholine receptors were detected using [^{3}H]-bungarotoxin. In fact, autoradiography detection of acetylcholine receptors (nicotinic, i.e., on motor endplate) started in 1970s of the twentieth century. In the same time, Kuhar and Yamamura have published the study on localization of muscarinic receptors (MRs) in the rat brain [9]. Shortly after, autoradiography of muscarinic and their counter-regulatory receptors, adrenoceptors [10] showed its localization on cardiomyocytes in culture. Then, muscarinic receptors were detected in the retina [11], in presynaptic nerve terminals in the heart [12], and repeatedly in the central nervous system (for review *see* [13]). Less work was devoted to characterize muscarinic receptors in peripheral tissue like bladder [14]. Some snake toxins, that are more selective among muscarinic receptor subtypes, were radiolabeled with aim to prepare subtype specific ligand [15]. The main disadvantage of snake toxins is irreversibility of binding and not well-defined allosteric binding [15, 16]. Also, uncertain effects were revealed on adrenoceptors [15]—there is discrepancy between inhibited prazosin binding and abolishment of such binding by atropine: muscarinic toxins can also inhibit the binding of [^{3}H]-prazosin, an antagonist of α-adrenergic receptors. But, binding of radioactive toxins to rat brain was completely abolished by atropine, indicating that the toxins target only muscarinic receptors.

2 Principles of Receptor Autoradiography

Depending on the degree of anatomical resolution, autoradiography can be divided into micro-autoradiography (using exposure and development of photographic emulsion visualized by microscopic technique at cellular and subcellular level) and macro-autoradiography (using X-ray or autoradiography films to produce radioisotope distribution images with resolution at macroscopic level) [6, 7]. The detection and visualization of radioligand tissue distribution throughout the whole body at the level of organs and organ systems is called whole-body macro-autoradiography [7].

In general, there are two ways, how to detect the receptors with radioactive ligands. First is in vivo autoradiography when the receptors are labeled within intact living tissue by systemic or intracerebral administration of radioligand and distribution of radiolabeled receptors within the specimen is then determined ex vivo either by micro or macro-autoradiography [3, 7].

The idea of in vivo labeling of receptors and their visualization gave rise to development of noninvasive in vivo imaging techniques such as positron emission tomography (PET) and single photon emission computed tomography scanning (SPECT, [3]). For detailed description of PET method *see* Chapter 10. Second is in vitro autoradiography [17, 18], that uses slide-mounted tissue sections which are incubated with radioligand what is subject of this chapter. In vitro autoradiography offers several advantages over the in vivo autoradiography. These includes reduced amounts of the radioligand, precise control of the radioligand binding conditions (incubation buffer, pH, incubation temperature and time, exact concentration of the radioligand, duration and number of washings to remove unbound radioligand), use of ligands that do not cross blood–brain barrier or are not metabolically stable, ability to perform competition assays with unlabeled ligands and saturation studies in addition of regional mapping of the ligand binding sites [3, 19].

In principle, the receptor binding of radioactive substance in vitro autoradiography is not different from the radioligand binding to membranes or homogenates (*see* Chapter 3): The radiolabeled compound specific to a given receptor binds to the receptor and then free radioligand is separated.

While receptor autoradiography can provide valuable information about the distribution and density of receptor binding sites it does not evaluate their signaling capacity. In case of distinct G protein-coupled receptors (GPCRs) a specialized in vitro receptor autoradiography was developed to address this issue. While preserving the high degree of anatomical resolution, [^{35}S]GTPγS binding autoradiography, also known as functional receptor autoradiography, was developed [20]. This technique combines the advantages of classical in vitro receptor autoradiography and

[^{35}S]GTPγS binding assay on cell membranes to provide information about signaling capacity – functional state of GPCRs at high anatomical resolution. The aim of receptor autoradiography is visualization and quantification of the binding sites of a given receptor. By contrast functional autoradiography aims to visualize the downstream signaling event upon agonist stimulation. In detail, this method studies CNS distribution of [^{35}S]GTPγS binding under agonist stimulation in the presence of GDP (suppress basal binding—*see* [20] for details) and Mg^{2+} (shifts the equilibrium towards the high-affinity state of receptor). Specificity of binding should be confirmed by antagonizing effects of atropine (in case of MRs). Thus only those potentially active GPCRs (i.e., those receptor-G protein complexes that are still able to function in tissue sections) are recruited and visualized in functional autoradiography. For detailed description of this method, its advantages and limitations *see* [20].

The basic principle of any autoradiography is creation of an image that specifically shows distribution of the radioligand binding within the specimen, the autoradiogram. The radioactive decay of radiolabeled ligand that is bound to a protein or nucleic acid generates changes in detection media that can be autoradiography film exposed directly to the radioactive decay, direct exposure with an intensifying screen [1, 21] and fluorography exposure (fluorography, that is not subject of this chapter) [17]. There are multiple methods how to detect radioactivity in situ: the film autoradiography, the electronic autoradiography, and the biomaging/phosphor imaging. Based on the way how autoradiogram is acquired autoradiography can be divided into direct and indirect autoradiography. A typical example of direct autoradiography is contact film autoradiography when ionizing radiation, that is emitted by the radioligand, is detected by autoradiography film to generate a latent image. Then the autoradiogram is developed by photographic processing of the film. In indirect autoradiography such as phosphor imaging or the use of trans-screens where the radioactive signal is first converted into the light which is subsequently detected with phosphor imager or autoradiography film to generate digitalized autoradiogram or latent image, respectively.

The isotopes usually used in autoradiography determination are listed in Table 1.

For further use we will focus on the in vitro autoradiography of receptors, with specific aim to describe in vitro autoradiography of muscarinic receptors.

2.1 Film Autoradiography

There is a broad range of commercially available films that can be used in autoradiography to detect directly or in conjunction with intensifying screens or trans-screens the radiation within the specimen (e.g., Kodak, Amersham (GE Healthcare)). The selection of autoradiography film type depends on the radioisotope used in the assays, the way of exposure, importance of sensitivity, resolution and speed of detection [2, 21].

Table 1
Radioligands of choice and their half-lives, specific activity (SA), maximal energy, tissue range, and decay

Radionuclide	Half-life	Maximal specific activity (Ci/mol)	Decay mode	Energy (max.) (MeV)	Max. tissue range	Application
^{14}C	5730 years	6.7×10^{1}	β	0.156	0.008	1, 2, 3, 4, 5, 6
^{3}H	12.43 years	2.9×10^{4}	β	0.0186	0.301	4, 5
^{35}S	87.4 days	1.5×10^{6}	β	0.167	0.042	1, 2, 3, 4, 5, 6
^{32}P	14.3 days	9.2×10^{6}	β	1.709	2.750	1, 2, 3
^{125}I	60.0 days	2.2×10^{6}	γ	0.035	0.019	5, 6
^{131}I	8.04 days	1.6×10^{7}	β	0.364	2.300	5

Notes (explanation of Application legend): 1: Southern blots, 2: Northern blots, 3: DNA sequencing, 4: Protein synthesis, 5: In situ hybridization, 6: Western blots
Adapted from refs. [17, 2, 19]

Based on the type of exposure method, film autoradiography can be divided into direct and indirect film autoradiography. In direct exposure procedure, the radioactive specimen is directly apposed to autoradiography film in light-tight autoradiography cassette. In indirect type of exposure such as trans-screen intensifying-screen exposure, the radiolabeled specimen is tightly apposed to a medium that converts ionizing radiation into the light emission that is then detected by the autoradiography film. Converting ionizing radiation to light greatly increases detection efficiency [2, 21].

A typical autoradiography film is composed of a polyester support (clear or colored) that is coated either on one side or on both sides by emulsion of light-sensitive silver halide grains and gelatin. The emulsion layers are then protected by an anti-scratch layer. When the photographic emulsion is exposed to ionizing radiation the silver ions are converted into the silver atoms to produce a stable latent image. In subsequent film processing these few silver atoms catalyze the reduction of the silver halide crystal to metallic silver to produce visible image of the radioisotope distribution within the specimen [2, 21].

Single-coated autoradiography films (e.g., Biomax MR) are optimized for detection of medium-energy radioisotopes (e.g., ^{14}C, ^{35}S, and ^{33}P) in direct exposure mode. When used with high-energy isotopes (e.g., ^{125}I, ^{32}P) they provide maximum resolution. However, because of the anti-scratch protective layer, they are not suitable for detection of ^{3}H (what is the case of muscarinic receptor ligands) [1, 21]. ^{3}H is a β-emitter with low energy, that has only limited permeability through the protective layer to expose the photographic emulsion. Therefore specialized film lacking the overcoat layer and thus allowing direct contact of ^{3}H emission with photographic emulsion has to be used. Then, a special attention

has to be paid to handling these films to avoid their damage [19, 21]. The direct exposure is done at room temperature (RT) [21].

Alternatively, ^{3}H can be detected using trans-screen, intensifying screen system. In this type of exposure, the radioactive specimen is apposed to the surface of phosphor layer coated on a thin clear plastic base. The phosphor layer captures the beta particles and converts their energy to photons. Photons are then directed to the autoradiography film placed between the phosphor layer and reflecting layer. Films that are spectrally matched to the trans-screen are used. The optimum exposure temperature range (determined by experience) is –70 to –80 °C [21]. In general, detection of emitted light is significantly improved by reducing the exposure temperature. The latent image center forming in the silver grain becomes more stable, thus reducing latent-image fading (signal loss). The detection sensitivity increases because the latent image accumulates with additional light exposure.

The conversion of ionizing radiation to light emissions is also the principle of intensifying screen exposure. Intensifying screens greatly increase the sensitivity and speed of detection. In this type of exposure, the radiolabeled specimen is placed in direct contact with one side of double-coated autoradiography film and intensifying screen is apposed to the other side of the film. The radioisotope must have sufficient energy (e.g., ^{32}P, ^{125}I) to pass through the autoradiography film before reaching the intensifying phosphors in the screen. The ionizing radiation (γ-rays and high energy β-particles) is then converted by the screen into the light emission that is detected by the film. The optimum exposure temperature range is –70 to –100 °C [1, 21].

Impregnation of the radiolabeled specimen with a scintillator to convert ionizing radiation to light emission and thus enhance detection efficiency by autoradiography film is called fluorography. Fluorographic exposure is used for detection of low- and medium-energy radioisotopes such as ^{3}H, ^{14}C, and ^{35}S. The optimum exposure temperature range is –70 to –100 °C [1, 2, 21].

It is necessary to perform three steps when detecting radioligand distribution within the specimen using film autoradiography: direct or indirect exposure of radiolabeled specimen to the autoradiography film, film development at the end of exposure and evaluation of autoradiograms. The length of exposure for a given radioligand is subject to preliminary experiments. This time depends on the type of radioisotope and radioactivity amount applied to specimen [18, 21]. It is necessary to expose sensitive film to calibrated amount of radioactivity. If the autoradiography resolution is comparable to that of the original chromatogram, the exposition is properly done [17].

Autoradiograms obtained by film autoradiography are analyzed by film densitometry using computer-assisted densitometric systems. Quantification of radioactivity amount bound to the protein

(nucleic acid) requires comparison of the measured optical density to a radiation response curve generated using standards on the same media (film, or storage phosphor screen as mentioned below) [17, 19]. Standards can be purchased as radiolabeled plastic polymers. Alternatively, it is possible to prepare standards by labeling tissue paste homogenates or plastics with defined amounts of radioisotope. The apparent disadvantage of autoradiography films is their narrow linear dynamic range of response. The relationship between incident-radiation exposure and optical density is however linear only over limited range. Eventually the media can be saturated and will not be more sensitive to additional exposure. In such cases, the analysis of autoradiograms is not possible. As a result, multiple exposures of the same specimen are often required [19] to determine optimal exposure time. Exposure time depends on the type of isotope and amount of radioactivity applied to the plate. In case of film autoradiography, both the narrow linear dynamic range (from 300 to 1) of the method (when using image analysis) and the lack of sample preservation (in zonal analysis) constitute a definite disadvantage. The linear dynamic ranges of the phosphor image technique are wider (by at least 10^5) than is needed for detection in film autoradiography.

Film development can be made automatically using fully automated benchtop film processors or manually in tanks and trays using film developers and fixators. In principle, developing, rinsing, fixing, washing, and drying are five steps of this process, and the freshness of chemicals is a critical point that can affect the quality of results. For details on manual processing of autoradiography films please *see* ref. 21.

2.2 Bioimaging/ Phosphor Imaging

Storage phosphor screen imaging technology was introduced by Fuji Company in 1980s of the twentieth century. Now, after more than 30 years, other suppliers of this material are on the market (e.g., GE Healthcare, Perkin Elmer, Bio-Rad). The exposition time in phosphor imaging is approximately 1 week, while in classical film autoradiography it is as long as several weeks. This method is similar to film autoradiography but has some advantages, mainly shortening of exposition time (in comparison to working with tritium labeled compounds). In some papers, this type of autoradiography is called "filmless autoradiography" referring to usage of other medium than film.

Phosphor imaging technique uses storage phosphor screens to detect and store energy of ionizing radiation in a stable state to generate latent images of the distribution of radioisotopes within the specimen. Phosphor imaging screens consists of support, photostimulatable phosphor layer (crystals of $BaFBr:Eu^{2+}$) and protective layer. These crystals are able to store the energy in crystal vacancies when irradiated. Then the luminescence occurs, that is evoked by change of Eu^{2+} ions into Eu^{3+} that leads to electron release.

Electrons are trapped in the Br vacancies and color centers are formed [17]. Screens with protective layer are suitable for detection of radioisotopes such as ^{32}P, ^{125}I, ^{35}S, ^{33}P, and ^{14}C, but not for ^{3}H. Similarly to autoradiography film, ^{3}H signal has to be directly accessible to photo-sensitive phosphor layer and imaging plates constructed without protective coat has to be used.

For exposure with phosphor imaging screens, the radioactive specimen is directly apposed to the phosphor screen in light-tight autoradiography cassette. After exposure, latent images are developed and digitized using phosphor imager. The screen is removed from autoradiography cassette under safe-light conditions and placed into the phosphor imager for reading. During scanning the phosphors are activated by a laser beam (633 nm) that leads to the release of stored energy as luminescence. The intensity of released luminescence is proportional to the amount of radioactivity in the specimen. The luminescence is recorded and stored in relation to the position of the laser beam to generate images that are then displayed on video monitor. The stored images are subsequently analyzed with an appropriate software [1].

Phosphor imaging technique offers several advantages over the film autoradiography. These include a linear dynamic range over five orders of magnitude (1.5 orders of magnitude in case of film), higher sensitivity (up to 100 times, depending on sample type and radioisotope used), and reduced exposure times (up to one-tenth, depending on sample type and radioisotope used) [1, 22]. The high sensitivity and wide linear dynamic range allows to detect and analyze weak and strong signals simultaneously. The results come out already in digitized form, which facilitates analysis of autoradiograms. Unlike autoradiography film, storage phosphor screens with protective layer can be used repeatedly if handled carefully. Unfortunately this is not the case for ^{3}H sensitive screens, which lack the protective layer and can be easily contaminated or damaged by exposure to the specimen. However, when ^{3}H sensitive screens are used with thin tissue sections mounted on glass-slides, the surface of the screen that has not been in contact with radiolabeled tissue section can be reused.

The most but not all of stored information is released upon scanning with the phosphor imager. For further use of the screen, the remaining signal must be erased with bright visible light (there are commercially available erasers). This is an important step that cannot be omitted as not properly erased screen retains images from previous exposure that can interfere with the image actually analyzed.

2.3 Electronic Autoradiography

This technique differs from previously mentioned one in the absence of storage medium. The radioactivity is measured directly with imaging detectors. Berthold's digital autoradiograph and Instant-imager (Canberra-Packard) are used for these purposes.

The principle of digital autoradiograph is based on measuring position and intensity of two-dimensional distributions of ionizing radiation on the surface (thin-layer chromatography plate) [17].

Instant imager consists of two sections [17], the microchannel array plate and a multiwire chamber and is continuously flowed by gas (argon, CO_2, and isobutene). The principle is based on gas ionization in one of the microchannels by beta-particle which is emitted from a source of radioactivity. This leads to the production of electrons, that are accelerated by the high electric field in the microchannel. This process leads to the further gas ionization and production of electron cloud, that migrates up an electric field gradient into the multiwire chamber.

3 Advantages and Disadvantages of Method

The principle of ligand binding to receptors is same as in radioligand binding studies. But, there are some advantages of autoradiography method in comparison to binding studies. While radioligand binding studies are restricted to the brain areas that can be precisely dissected, in vitro autoradiography allows explore radioligand binding to MRs in very well-defined brain regions. In case of smaller brain areas or regions with lower MR density it is necessary to pool tissue from more animals. In addition, binding in homogenates/membrane fractions is limited by the density of MR in the sample. By contrast, in vitro autoradiography has high sensitivity allowing explore brain regions even with few MR. The use of very thin tissue sections in vitro autoradiography provides several advantages over the large tissue blocks used in binding studies in homogenates/membrane fractions. The brain sectioning allows analyzing MR density in virtually all brain areas of a single animal greatly reducing the number of experimental animals. Moreover, sectioning of a single brain generates sufficient number of tissue sections to explore the binding of multiple radioligands in a particular brain area of the same animal. This further reduces the number of experimental animals and allows comparing the effect of treatment on multiple targets (receptors, transporters) in a single animal.

The important question, also discussed in the chapter on Radioligand binding, is the selectivity of radioligand used in the experiments. A general problem in identification of muscarinic receptor subtypes present in specific central nervous system area is the lack of highly subtype-selective muscarinic antagonists. The muscarinic receptor subtypes affinities for pirenzepine and AFDX-384 are shown in Table 2. It can be deduced from this table that both pirenzepine and AFDX-384 has high affinity not only for M_1, M_2 muscarinic receptors, respectively, but also for M_4 muscarinic receptor subtype. In radioligand binding studies, it is therefore

Table 2
Pirenzepine and AFDX-384 affinity constants (log affinity or pKi values) for muscarinic receptor subtypes

Antagonist	Receptor subtype				
	M_1	M_2	M_3	M_4	M_5
Pirenzepine	7.8–8.5	6.3–6.7	6.7–7.1	7.1–8.1	6.2–7.1
AF-DX 384	7.3–7.5	8.2–9.0	7.2–7.8	8.0–8.7	6.3

Data were obtained from ref. [35]

necessary to use a combination of various antagonists. However, for autoradiography detection this approach is not suitable because of evaluation limitations of such changed "binding." Thus, the present protocols for M_1 and M_2 muscarinic receptor subtypes identification should be considered as method for detection of M_1 (or M_2) and also small portion of M_4 muscarinic receptors. Unfortunately, only few papers report these binding sites as M_1/M_4 muscarinic receptors (e.g., [23, 24]).

Historically, tritiated pirenzepine was used as ligand that binds to muscarinic receptors with distinct binding in specific brain areas [25]. Further, distinct distribution was found in the central nervous system. [^{3}H]-QNB and [^{3}H]-pirenzepine both label regions of the cerebral cortex, hippocampus, striatum, and dorsal horn of the spinal cord, while sites in the cerebellum, nucleus tractus solitarius, facial nucleus, and ventral horn of the spinal cord are labeled with [^{3}H]-QNB and not by [^{3}H]-pirenzepine [26]. These observations indicated binding to different subtypes of muscarinic receptors. This was further expanded to definition of binding sites as M_1 muscarinic receptors [27] and in the middle of 1980s pirenzepine binding sites were considered as M_1 muscarinic receptors [28, 29]. On the other hand, AFDX-384 was from the beginning considered as M_2 muscarinic receptor specific ligand [30] and some authors became aware of limited selectivity (e.g., [31]). In many cases, however, [^{3}H]-AFDX-384 and [^{3}H]-pirenzepine are considered as selective ligands [32, 33].

4 Equipment, Materials, and Setup

Before the start of work it is necessary to prepare all equipment, surgical instruments, buffers, and all other things that are essential for the method. Appropriate preparation is a basic condition for successful work. Some details about items listed below are discussed in other sections of this chapter.

The items are as follows:

Items for tissue dissection and preparation of glass slide-mounted tissue sections:

1. Target tissue (mice or rat brain). For tissue preparation *see* Section 5.
2. Surgical instruments (e.g., tweezers, forceps, scissors).
3. Gelatine-coated standard microscope glass slides (25 × 5 mm) with frosted ends allowing marking of individual slides or ready to use glass slides treated by manufacturer to attract and firmly bind frozen tissue sections without additional coating of the glass-slide surface (e.g., Superfrost® Plus glass slides).
4. Pencil (for labeling the glass slides).
5. Paintbrush (flat or round with small diameter, for tissue manipulation).
6. Parafilm.
7. Dry ice (better supplied as powdered dry ice).
8. Polystyrene box (for freezing the freshly dissected tissue).
9. Cryostat operating between −10 and −25 °C (e.g., Leica CM3050S).
10. Tissue glue matrix (e.g., Tissue OCT from Labonord).
11. Slide boxes.
12. Desiccant (silica gel with an indicator of moisture content).
13. Isopentane.
14. Brain atlas (e.g., very useful is Paxinos' atlas [34]).

Items for preparation of gelatin-coated microscope glass slides:

15. Gelatin.
16. Chromium(III) potassium sulfate dodecahydrate ($KCr(SO_4)\cdot 12H_2O$.
17. Distilled water.
18. Paper filter.
19. Glass funnel.
20. Slide boxes.
21. Desiccant.

Items for specific labeling of MR in brain sections:

22. Liquid scintillation counter (e.g., Beckman Coulter).
23. Scintillation vials.
24. Scintillation cocktail (e.g., GE Healthcare Life Sciences or homemade (see below)).
25. Pieces of glass fiber filter paper.
26. Hair dryer operating at room temperature.

27. Slide staining set (staining dishes, slide holder).
28. Drain rack.
29. Polystyrene box.
30. Crushed ice.
31. Distilled water.
32. 50 mM sodium/potassium phosphate buffer, pH = 7.4.
33. Atropine sulfate.
34. Radioligands ([^{3}H]-QNB and [^{3}H]-NMS, [^{3}H]-pirenzepine, and [^{3}H]-AFDX-384).

    Items for preparation of liquid scintillation cocktail:

35. Naphthalene.
36. 2,5-Diphenyloxazole (PPO).
37. 1,4-Bis(5-phenyl-2-oxazolyl)benzene (POPOP).
38. Methanol.
39. Ethylene glycol.
40. 1,4-Dioxane.

    Items for receptor binding evaluation:

41. ^{3}H sensitive storage phosphor screen (e.g., storage phosphor screen BAS IP-TR).
42. Phosphor imager (e.g., Typhoon FLA7000 biomolecular imager).
43. PC with WinXP or Win7 for results evaluation using specific software.
44. Computer-assisted densitometric system (e.g., MCID).
45. Suitable tritium standards on glass slides (e.g., American Radiolabeled Chemicals).
46. Light-tight autoradiography exposure cassette (e.g., Carestream Kodak Biomax).
47. Cartridge paper.
48. Double-sided tape.

5 Procedures

Here we will provide protocols for muscarinic receptors determination using four radioligands: unspecific [^{3}H]-QNB (*see* Fig. 1) and [^{3}H]-NMS (*see* Fig. 2), M_1 specific [^{3}H]-pirenzepine (*see* Fig. 3) and M_2 specific [^{3}H]-AFDX-384 (*see* Fig. 4). In our laboratory we use storage phosphor screen imaging technology and thus this technique is described further.

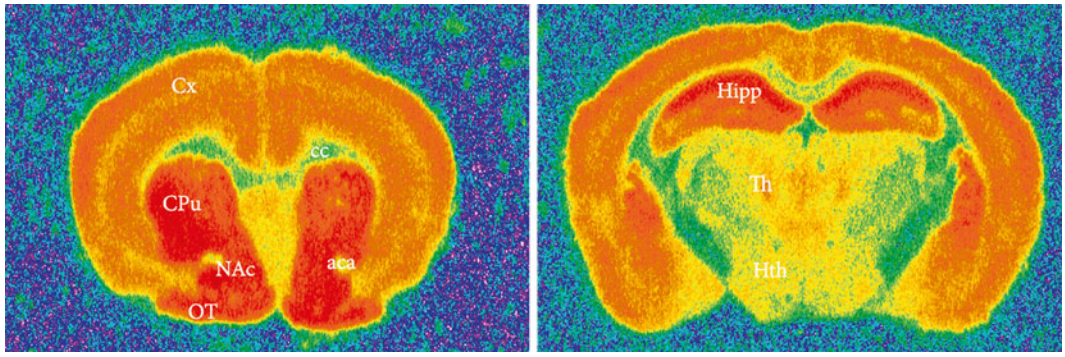

Fig. 1 Illustrative autoradiograms of [^{3}H]-QNB binding in coronal brain sections in wild type mice. *Aca* anterior commissure, anterior part, *cc* corpus callosum, *CPu* caudate putamen, *Cx* cortex, *Hipp* hippocampus, *Hth* hypothalamus, *OT* olfactory tubercle, *Th* thalamus

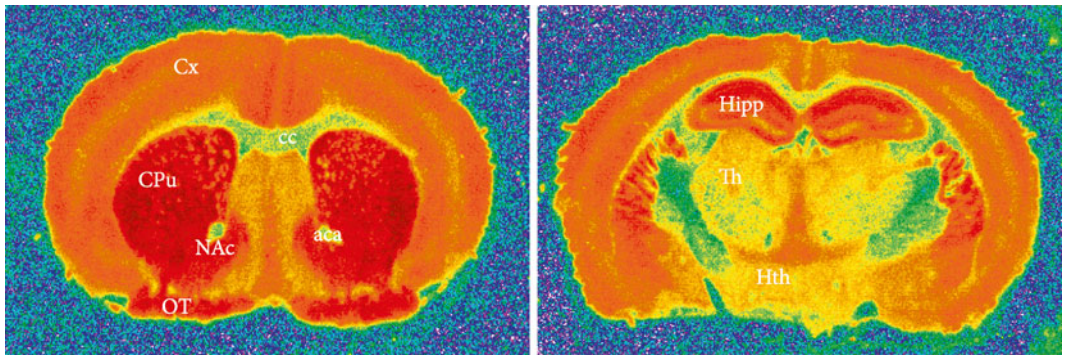

Fig. 2 Illustrative autoradiograms of [^{3}H]-NMS binding in coronal brain sections in wild type mice. *Aca* anterior commissure, anterior part, *cc* corpus callosum, *CPu* caudate putamen, *Cx* cortex, *Hipp* hippocampus, *Hth* hypothalamus, *OT* olfactory tubercle, *Th* thalamus

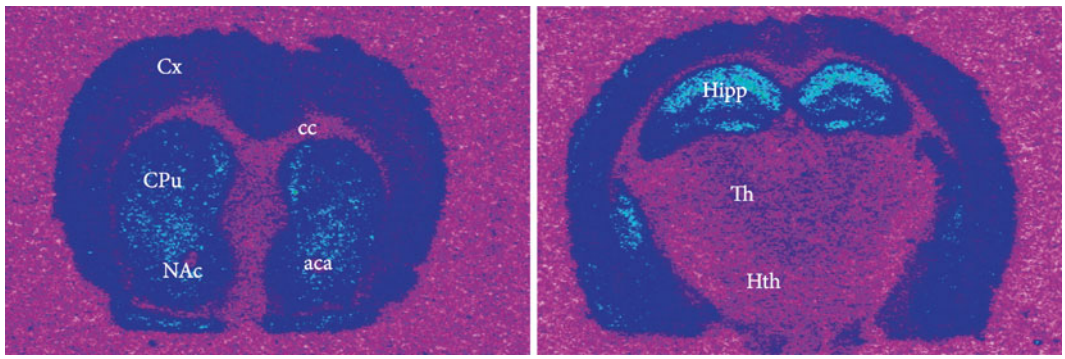

Fig. 3 Illustrative autoradiograms of [^{3}H]-pirenzepine binding in coronal brain sections in wild type mice. Note the barely visible labeling in Th and Hth, brain areas in which M_1 are practically absent. *Aca* anterior commissure, anterior part, *cc* corpus callosum, *CPu* caudate putamen, *Cx* cortex, *Hipp* hippocampus, *Hth* hypothalamus, *OT* olfactory tubercle, *Th* thalamus

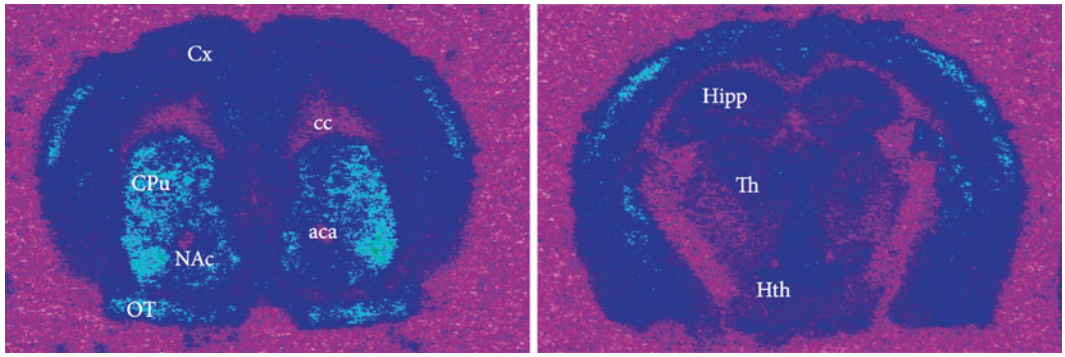

Fig. 4 Illustrative autoradiograms of [^{3}H]-AFDX-384 binding in coronal brain sections in wild type mice. *Aca* anterior commissure, anterior part, *cc* corpus callosum, *CPu* caudate putamen, *Cx* cortex, *Hipp* hippocampus, *Hth* hypothalamus, *OT* olfactory tubercle, *Th* thalamus

In vitro autoradiography of brain muscarinic receptors (MR) is a powerful tool to assess the distribution and MR changes in a variety of experimental models (drug treatment, genetic manipulations, ontogenetic studies) at a high degree of anatomical resolution and reproducibility of results.

Previously the apparent disadvantage of in vitro autoradiography of MR using [^{3}H]-labeled compounds and standard [^{3}H]-sensitive autoradiography films was the time of exposure of radiolabeled sections to the films to detect the bound radioactivity and generate autoradiogram, which could take as long as several weeks. Nowadays, the use of phosphor imaging techniques overcomes this issue and autoradiography of MR can be completed within 1 week.

Similarly to in vitro autoradiography of other receptors, in vitro autoradiography of MR consists of three major steps.

1. Tissue processing and preparation of glass slide-mounted tissue sections.
2. Preincubation, incubation of sections with appropriate radioligand and washing.
3. Detection, visualization and analysis of autoradiographic signal.

5.1 Tissue Processing and Preparation of Glass Slide-Mounted Tissue Sections

1. Sacrifice experimental animal according to the regulations concerning the handle and use of laboratory animals.
2. Rapidly remove the brain from the skull and immediately freeze the brain in isopenthane cooled to −30 °C. Alternatively put the brain on the piece of parafilm and place it on powdered dry ice in a closed polystyrene box. The rapid processing of fresh tissue prevents or minimizes the postmortem loss of receptor-binding sites.

3. If the brains are not directly used for cryosectioning, store the brains at −80 °C. Before cryosectioning of brains stored at −80 °C, transfer brains from −80 to −20 °C for 3 h.
4. Attach the brain to the specimen disc that holds the specimen during sectioning (cryostat chuck).
5. Cover the cryostat chuck with a layer of tissue glue matrix and place it into the quick freeze shelf inside the cryostat chamber.
6. If the cryostat is not equipped with system that secures rapid freezing of the disc, perform the mounting of the brain to the chuck inset into the powdered dry ice.
7. Choose the right orientation of the brain for sectioning of coronal, sagittal or axial brain slices. Always use steel tweezers cooled to the cryostat temperature to manipulate with brain.
8. Once the glue begins to freeze immerse the brain into the glue perpendicular to the chuck. Within few seconds the glue matrix is frozen. Subsequently you can add an additional layer of glue to secure the firm fixation of the brain during the sectioning.
9. Insert the specimen disc with fixed brain into the specimen head. The optimal temperature of the cutting is usually between −15 and −20 °C. The temperature within cryostat chamber and temperature of specimen strongly influences the quality of sections. The appropriate temperature should be set in preliminary experiments.
10. Trim the brain to the anatomical level corresponding to your brain area of interest. Set the appropriate thickness of sections and sectioning speed (in case of motorized devices). When sectioning manually, rotate the hand wheel evenly and at uniform speed. It is recommended to discard first 2–3 sections before tissue section collecting. The most common section thickness is 16 μm. Thinner sections can be cut to collect more sections through a desired brain region.
11. Cut the brain section of appropriate thickness. The tissue section will remain on the knife or knife holder. Use paintbrush to manipulate with section and make it accessible to the glass slide.
12. Thaw and mount the section at the bottom of the glass slide. Place the glass slide of RT over the section as closely as possible. The section will stick to the glass slide. Dry the section at room temperature. Store the dried sections in the slide boxes with desiccant at −80 °C.

Typically four sections are collected on one glass slide. To increase the homogeneity of samples collect every fifth or tenth section on an individual slide (depending on the size of brain area). For brain areas that span several hundred micrometers through the brain (e.g., striatum, dorsal hippocampus) collect brain sections on a set of ten

slides. During the collecting sections keep the slides at RT. Thaw mount the first section on the first slide, the second section on the second slide and the tenth section on the last slide. Collect the next ten sections in the same way (thaw mount the 11th section on the first slide, 12th on the second slide, etc.). Collect another two sets of sections. Finally, at individual slide you will have four sections while each section will be 160 μm distant from the previous one.

Recipe 1. Preparation of gelatin-coated microscope glass slides

1. Dissolve 10 g of gelatin in 1 L of distilled water at 60 °C.
2. Dissolve $KCr(SO_4)\cdot 12H_2O$ in gelatin solution chilled to RT.
3. Filter the solution through the paper filter.
4. Store at RT in a dark place.
5. Dip slides into the gelatin solution for 5 min.
6. Dry slides for 24 h at 37 °C in the presence of desiccant
7. Store slides in slide boxes containing desiccant in a dry place.

5.2 Specific Labeling of MR in Brain Sections

Each assay consists of four major steps:

1. Pre-incubation of tissue sections to remove endogenous ligands.
2. Incubation of tissue sections in incubation medium comprising the particular radioligand.
3. Washing of tissue sections to remove unbound radioligand from tissue.
4. Rapid drying of labeled sections to prevent diffusion of radioligand bound to receptors.

Steps 1–3 are described in detail below:

1. Prepare five staining dishes. Fill one with maximal volume of pre-incubation medium, the second one with incubation medium containing radioligand at appropriate concentration at suitable volume. The volume of incubation medium is chosen to following two conditions: First, it has to be sufficient to cover all tissue sections. Second, the concentration of radioligand in incubation medium should be only marginally affected by binding. This can be experimentally addressed by sampling the incubation medium before, during and after incubation and determining concentration of free radioligand by liquid scintillation counting. Concentration of free radioligand should not differ among determinations.
2. Shortly before the end of incubation period fill two dishes with ice-cold washing medium and one with ice-cold water. Place the dishes containing ice-cold solutions into the ice in polystyrene box to maintain their temperature.

Recipe 2. Preparation of liquid scintillation cocktail

1. Add 120 g of naphthalene, 8 g of PPO and 0.4 g of POPOP to a beaker.
2. Add 500 ml of dioxane, 200 ml of methanol and 40 ml of ethylene glycol to a beaker.
3. Stir until naphthalene dissolves (ca. 30 min).
4. Add 1260 ml of dioxane and stir for 2 h.

Detailed protocols for above mentioned radioligands are in further sub-sections.

5.2.1 Labeling of MR with [^{3}H]-QNB

1. Remove the slide-mounted tissue sections from the freezer and allow them to thaw and dry for 20 min at RT. Transfer the slides into the slide holder.
2. Pre-incubate dried sections for 30 min in 50 mM sodium/potassium phosphate buffer (pH 7.4) at RT (pre-incubation medium).
3. Transfer the sections into the fresh 50 mM sodium/potassium phosphate buffer (pH 7.4) containing 2 nM [^{3}H]-QNB (incubation medium) and incubate for 2 h at RT.
4. To determine nonspecific binding of [^{3}H]-QNB, label adjacent sections with incubation medium supplemented with 10 μM atropine (final concentration) sulfate in the medium.
5. Wash the sections for 5 min in ice-cold 50 mM sodium/potassium phosphate buffer (pH 7.4).
6. Wash the sections second time for 5 min in fresh ice-cold 50 mM sodium/potassium phosphate buffer (pH 7.4).
7. Dip the slides for 2 s in ice-cold distilled water.
8. Immediately place the slides upright in the drain rack with tissue sections on the top and dry sections with gentle stream of room temperature air.
9. Store the dried section in slide boxes containing desiccant.

5.2.2 Labeling of MR with [^{3}H]-NMS

1. Remove the slide-mounted tissue sections from the freezer and allow them to thaw and dry for 20 min at RT. Transfer the slides into the slide holder.
2. Pre-incubate dried sections for 30 min in 50 mM sodium/potassium phosphate buffer (pH 7.4) at RT.
3. Transfer the sections into the fresh 50 mM sodium/potassium phosphate buffer (pH 7.4) containing 2.5 nM [^{3}H]-NMS and incubate for 1 h at RT.
4. To determine nonspecific binding of [^{3}H]-NMS, label adjacent sections with incubation medium supplemented with 10 μM atropine (final concentration) in the medium.

5. Wash the sections for 5 min in ice-cold 50 mM sodium/potassium phosphate buffer (pH 7.4).
6. Wash the sections second time for 5 min in fresh ice-cold 50 mM sodium/potassium phosphate buffer (pH 7.4).
7. Dip the slides for 2 s in ice-cold water.
8. Immediately place the slides upright in the drain rack with tissue sections on the top and dry sections with gentle stream of room temperature air.
9. Store the dried section in slide boxes containing desiccant.

5.2.3 Labeling of MR with [^{3}H]-pirenzepine

1. Remove the slide-mounted tissue sections from the freezer and allow them to thaw and dry for 20 min at RT. Transfer the slides into the slide holder.
2. Pre-incubate dried sections for 30 min in 50 mM sodium/potassium phosphate buffer (pH 7.4) at RT.
3. Transfer the sections into the fresh 50 mM sodium/potassium phosphate buffer (pH 7.4) containing 5 nM [^{3}H]-pirenzepine and incubate for 1 h at RT.
4. To determine nonspecific binding of [^{3}H]-pirenzepine, label adjacent sections with incubation medium supplemented with 10 μM atropine sulfate (final concentration) in the medium.
5. Wash the sections for 5 min in ice-cold 50 mM sodium/potassium phosphate buffer (pH 7.4).
6. Wash the sections second time for 5 min in fresh ice-cold 50 mM sodium/potassium phosphate buffer (pH 7.4).
7. Dip the slides for 2 s in ice-cold distilled water.
8. Immediately place the slides upright in the drain rack with tissue sections on the top and dry sections with gentle stream of room temperature air.
9. Store the dried section in slide boxes containing desiccant.

5.2.4 Labeling of MR with [^{3}H]-AFDX-384

1. Remove the slide-mounted tissue sections from the freezer and allow them to thaw and dry for 20 min at RT. Transfer the slides into the slide holder.
2. Pre-incubate dried sections for 30 min in 50 mM sodium/potassium phosphate buffer (pH 7.4) at RT.
3. Transfer the sections into the fresh 50 mM sodium/potassium phosphate buffer (pH = 7.4) containing 2 nM [^{3}H]-AFDX-384 and incubate for 1 h at RT.
4. To determine nonspecific binding of [^{3}H]-AFDX-384, label adjacent sections with incubation medium supplemented with 10 μM atropine sulfate (final concentration) in the medium.
5. Wash the sections for 5 min in ice-cold 50 mM sodium/potassium phosphate buffer (pH 7.4).

6. Wash the sections second time for 5 min in fresh ice-cold 50 mM sodium/potassium phosphate buffer (pH 7.4).
7. Dip the slides for 2 s in ice-cold distilled water.
8. Immediately place the slides upright in the drain rack with tissue sections on the top and dry sections with gentle stream of room temperature air.
9. Store the dried section in slide boxes containing desiccant.

5.3 Generation of Autoradiograms

1. Cut the cartridge paper to fit the autoradiography cassette.
2. Organize the slides and standard in a logical manner. Use double-sided tape to attach slides and standard to cartridge paper. In case that the size of microscope slide layer does not match that of the storage phosphor screen use additional microscope slides for covering of the free surface of the paper sheet to secure uniform contact of the screen.
3. Place the sheet with fixed slides into autoradiography cassette.
4. Appose the storage phosphor screen to the labeled sections and standard.
5. Close autoradiography cassette and note the date and time.
6. Expose storage phosphor screen for the predetermined period of time at RT.
7. After exposure, dim the lights and remove storage phosphor screen from the autoradiography cassette.
8. Scan the storage phosphor screen in a phosphor imager.
9. Save the digitized autoradiograms for further analysis.

5.4 Analysis of Autoradiograms

Proper analysis of autoradiograms requires reliable anatomical identification of brain regions of interest. This can be achieved in several complementary ways. In all cases, a detailed brain atlas is indispensable tool for identification of regional anatomy. The use of brain atlas by Franklin and Paxinos [34] is very useful, as it provides brain sections stained for acetylcholinesterase, which shows distribution pattern similar to that of MR. Autoradiograms in itself can be used to directly identify distinct brain regions. The heterogeneous distribution of MR binding sites within the tissue sections and thus signal intensity within corresponding autoradiogram can provide readily observable details and contrasts to directly identify many brain regions. As can be seen in Fig. 1 the white matter is virtually devoid of labeling and can be clearly distinguished from surrounding grey matter which shows different levels of labeling. Accordingly, the white matter structures and tracts such as internal capsule, corpus callosum, anterior commissure, fornix, and others can be clearly recognized. In addition there are significant differences in MR density between individual brain regions. For instance the density of MR in striatum is about twofold higher than that in cortex.

The anatomical identification of brain regions can be facilitated by conventional histology techniques such as Nissl staining. Either those radiolabeled and used for exposure or adjacent tissue sections can be processed for Nissl staining [19].

There is specialized software for analysis of digitized autoradiograms generated by phosphor imagers (e.g., MCID). The basic procedure for quantifying digitized autoradiograms with MCID Analysis is as follows:

1. Load the autoradiographic image file.
2. Establish a density calibration.
3. Use any Sample tool to gather data from tissue section(s).
4. Repeat steps 1–3 for all remaining image files.
5. Summarize and save the data.

6 Conclusions

In vitro autoradiography of MR is widely recognized method in neuroscience and neuropharmacology that can bring out unique information about the regulation of MR abundance under physiological as well as pathophysiological conditions (drug treatment, genetic manipulations, stress conditions, physiological processes like learning and memory and many others) at a high degree of anatomical resolution and reproducibility of results. The use of radioligand membrane binding techniques has been useful tool to determine pharmacological properties of wide range of receptors in the peripheral tissues as well as in the brain and is the method of choice for kinetic and competition assays. The apparent limitations of these techniques is however the resolution at the anatomical level. In particular, mapping the distribution of receptor binding sites in discrete functionally and/or anatomically defined regions of the brain is not possible by membrane binding techniques. While the use of radioligand membrane binding techniques is restricted to larger brain areas that can be precisely dissected, in vitro autoradiography allows exploring radioligand binding to MR in very discrete brain regions. In vitro autoradiography has high sensitivity allowing to explore brain regions even with few MR. The brain cryosectioning allows analyzing MR density in virtually all brain areas of a single animal greatly reducing the number of experimental animals. Moreover, cryosectioning of a single brain generates sufficient numbers of tissue sections to explore the binding sites of additional radioligands in a particular brain area of the same animal. Alternate sections collected during cryosectioning can be also processed in multiple assays such as in situ hybridization, histochemistry and functional autoradiography. This further reduces the number of experimental animals and allows comparing the effect of treatment on multiple targets (receptors, coupling of

receptors, transportes, mRNA, enzymes) in a single animal. There are multiple methods for detection and visualization of autoradiographic signal including sensitive media (film, screen) and media-free (electronic) autoradiography. As recommended method for this purposes, phosphor imaging with [^{3}H]-QNB and [^{3}H]-NMS, [^{3}H]-pirenzepine, and [^{3}H]-AFDX-384 is discussed in this chapter.

Acknowledgments

The research on this topic was supported by grant GAUK 328314 from Grant Agency of Charles University and by projects PRVOUK P25/1LF and PRVOUK P35/1LF.

References

1. Voytas D, Ke N (2001) Detection and quantitation of radiolabeled proteins and DNA in gels and blots. In: Frederick M Ausubel et al (eds.) Current protocols in molecular biology. Appendix 3: appendix 3A. doi:10.1002/0471142727.mba03as48
2. Laskey RA (1993) Efficient detection of biomolecules by autoradiography, fluorography or chemiluminescence. Principles of detection using radiographic film. Amersham Life Sci. Review 23:Part I
3. Chabot JG, Kar S, Quirion R (1996) Autoradiographical and immunohistochemical analysis of receptor localization in the central nervous system. Histochem J 28:729–745
4. de St Victor N (1867) Sur une noublle action de la lumière Sixième Mémoire. Hebdomadaire des Séances de l'Academie des Sciences 65: 505–507
5. Ross R (1966) Electron microscope autoradiography. Adv Tracer Methodol 3:131–137
6. Harvey B (2008) Autoradiography and fluorography. In: Rapley R, Walker J (eds) Molecular biomethods handbook. Humana, Totowa, pp 396–410. doi:10.1007/978-1-60327-375-6_26
7. Stumpf WE (2013) Whole-body and microscopic autoradiography to determine tissue distribution of biopharmaceuticals—target discoveries with receptor micro-autoradiography engendered new concepts and therapies for vitamin D. Adv Drug Deliv Rev 65:1086–1097. doi:10.1016/j.addr.2012.11.008
8. Porter CW, Barnard EA (1976) Ultrastructural studies on the acetylcholine receptor at motor end plates of normal and pathologic muscles. Ann N Y Acad Sci 274(1):85–107. doi:10.1111/j.1749-6632.1976.tb47678.x
9. Kuhar MJ, Yamamura HI (1975) Light autoradiographic localisation of cholinergic muscarinic receptors in rat brain by specific binding of a potent antagonist. Nature 253(5492): 560–561
10. Lane M-A, Sastre A, Law M, Salpeter MM (1977) Cholinergic and adrenergic receptors on mouse cardiocytes in vitro. Dev Biol 57(2): 254–269, doi:http://dx.doi.org/10.1016/0012-1606(77)90213-5
11. Sugiyama H, Daniels MP, Nirenberg M (1977) Muscarinic acetylcholine receptors of the developing retina. Proc Natl Acad Sci U S A 74(12):5524–5528
12. Hartzell HC (1980) Distribution of muscarinic acetylcholine receptors and presynaptic nerve terminals in amphibian heart. J Cell Biol 86(1):6–20
13. Hoss W, Messer W Jr (1986) Multiple muscarinic receptors in the CNS. Significance and prospects for future research. Biochem Pharmacol 35(22):3895–3901
14. Yoshida A, Fujino T, Maruyama S, Ito Y, Taki Y, Yamada S (2010) The forefront for novel therapeutic agents based on the pathophysiology of lower urinary tract dysfunction: bladder selectivity based on in vivo drug-receptor binding characteristics of antimuscarinic agents for treatment of overactive bladder. J Pharmacol Sci 112(2):142–150. doi:10.1254/jphs.09R14FM
15. Karlsson E, Jolkkonen M, Mulugeta E, Onali P, Adem A (2000) Snake toxins with high selectivity for subtypes of muscarinic acetylcholine receptors. Biochimie 82(9–10):793–806,

doi:http://dx.doi.org/10.1016/S0300-9084(00)01176-7

16. Olianas MC, Adem A, Karlsson E, Onali P (2004) Action of the muscarinic toxin MT7 on agonist-bound muscarinic M1 receptors. Eur J Pharmacol 487(1-3):65–72
17. Hazai I, Klebovich I (2003) Thin-layer radiochromatography. In: Sherma J, Fried B (eds) Handbook of thin-layer chromatography. Marcel Dekker, Inc., New York, pp 442–470
18. Kuhar MJ (2001) In vitro autoradiography. In: Enna SJ (editor-in-Chief) et al (eds.) Current protocols in pharmacology, Chapter 8:Unit 8.1. doi:10.1002/0471141755.ph0801s00
19. Frey KA, Albin RL (1997) Receptor binding techniques. In: Jacqueline N Crawley et al (eds.) Current protocols in neuroscience, Chapter1:Unit1.4.doi:10.1002/0471142301.ns0104s00
20. Sóvágó J, Dupuis DS, Gulyás B, Hall H (2001) An overview on functional receptor autoradiography using [35S]GTPgammaS. Brain Res Brain Res Rev 38:149–164
21. Bundy DC (2001) Autoradiography. In: John E Coligan et al (eds.) Current protocols in protein science, Chapter 10:Unit 10.11. doi:10.1002/0471140864.ps1011s10
22. Kanekal S, Sahai A, Jones RE, Brown D (1995) Storage-phosphor autoradiography: a rapid and highly sensitive method for spatial imaging and quantitation of radioisotopes. J Pharmacol Toxicol Methods 33:171–178
23. Zavitsanou K, Katsifis A, Mattner F, Huang X-F (2003) Investigation of M1//M4 muscarinic receptors in the anterior cingulate cortex in schizophrenia, bipolar disorder, and major depression disorder. Neuropsychopharmacology 29(3):619–625
24. Wang Q, Wei X, Gao H, Li J, Liao J, Liu X, Qin B, Yu Y, Deng C, Tang B, Huang XF (2014) Simvastatin reverses the downregulation of M1/4 receptor binding in 6-hydroxydopamine-induced parkinsonian rats: The association with improvements in long-term memory. Neuroscience 267:57–66, doi:http://dx.doi.org/10.1016/j.neuroscience.2014.02.031
25. Yamamura HI, Wamsley JK, Deshmukh P, Roeske WR (1983) Differential light microscopic autoradiographic localization of muscarinic cholinergic receptors in the brainstem and spinal cord of the rat using [3H]pirenzepine. Eur J Pharmacol 91(1):147–149, doi:http://dx.doi.org/10.1016/0014-2999(83)90379-5
26. Wamsley JK, Gehlert DR, Roeske WR, Yamamura HI (1984) Muscarinic antagonist binding site heterogeneity as evidenced by autoradiography after direct labeling with [3H]-QNB and [3H]-pirenzepine. Life Sci 34(14):1395–1402
27. Villiger JW, Faull RLM (1985) Muscarinic cholinergic receptors in the human spinal cord: differential localization of [3H]pirenzepine and [3H]quinuclidinylbenzilate binding sites. Brain Res 345(1):196–199, doi:http://dx.doi.org/10.1016/0006-8993(85)90854-6
28. Cortes R, Palacios JM (1986) Muscarinic cholinergic receptor subtypes in the rat brain. I Quantitative autoradiographic studies. Brain Res 362(2):227–238
29. Buckley NJ, Burnstock G (1986) Autoradiographic localization of peripheral M1 muscarinic receptors using [3H]pirenzepine. Brain Res 375(1):83–91, doi:http://dx.doi.org/10.1016/0006-8993(86)90961-3
30. Aubert I, Cecyre D, Gauthier S, Quirion R (1992) Characterization and autoradiographic distribution of [3H]AF-DX 384 binding to putative muscarinic M2 receptors in the rat brain. Eur J Pharmacol 217(2–3):173–184
31. Mulugeta E, Karlsson E, Islam A, Kalaria R, Mangat H, Winblad B, Adem A (2003) Loss of muscarinic M4 receptors in hippocampus of Alzheimer patients. Brain Res 960(1–2):259–262, doi:http://dx.doi.org/10.1016/S0006-8993(02)03542-4
32. Tien L-T, Fan L-W, Sogawa C, Ma T, Loh HH, Ho I-K (2004) Changes in acetylcholinesterase activity and muscarinic receptor bindings in μ-opioid receptor knockout mice. Molecular Brain Research 126(1):38–44, doi:http://dx.doi.org/10.1016/j.molbrainres.2004.03.011
33. Wolff SC, Hruska Z, Nguyen L, Dohanich GP (2008) Asymmetrical distributions of muscarinic receptor binding in the hippocampus of female rats. Eur J Pharmacol 588(2–3):248–250, doi:http://dx.doi.org/10.1016/j.ejphar.2008.04.002
34. Paxinos G, Franklin KBJ (2008) The mouse brain in stereotaxic coordinates. The coronal plates and diagrams, Compact edn, 3rd edn. Academic, London
35. Caulfield MP, Birdsall NJ (1998) International Union of Pharmacology. XVII. Classification of muscarinic acetylcholine receptors. Pharmacol Rev 50(2):279–290